Acta Crystallographica Section D
Biological Crystallography
ISSN 0907-4449

The first protein crystal structure determined from high-resolution X-ray powder diffraction data: a variant of T_3R_3 human insulin–zinc complex produced by grinding

R. B. Von Dreele,[a]* P. W. Stephens,[b] G. D. Smith[c] and R. H. Blessing[c]

[a]Manuel Lujan Jr Neutron Scattering Center, MS H805, Los Alamos National Laboratory, Los Alamos, NM 87545, USA, [b]Department of Physics and Astronomy, State University of New York at Stony Brook, Stony Brook, NY 11794-3800, USA, and [c]Hauptman-Woodward Medical Research Institute, 73 High Street, Buffalo, NY 14203-1196, USA

Correspondence e-mail: vondreele@lanl.gov

Received 26 June 2000
Accepted 4 October 2000

PDB References: T_3R_3 insulin–zinc complex, 1fub; T_3R_3DC insulin–zinc complex, 1fu2.

X-ray diffraction analysis of protein structure is often limited by the availability of suitable crystals. However, the absence of single crystals need not present an insurmountable obstacle in protein crystallography any more than it does in materials science, where powder diffraction techniques have developed to the point where complex oxide, zeolite and small organic molecular structures can often be solved from powder data alone. Here, that fact is demonstrated with the structure solution and refinement of a new variant of the T_3R_3 Zn–human insulin complex produced by mechanical grinding of a polycrystalline sample. High-resolution synchrotron X-ray powder diffraction data were used to solve this crystal structure by molecular replacement adapted for Rietveld refinement. A complete Rietveld refinement of the 1630-atom protein was achieved by combining 7981 stereochemical restraints with a 4800-step ($d_{\min}$ = 3.24 Å) powder diffraction pattern and yielded the residuals $R_{\rm wp}$ = 3.73%, R_p = 2.84%, R_F^2 = 8.25%. It was determined that the grinding-induced phase change is accompanied by 9.5 and 17.2° rotations of the two T_3R_3 complexes that comprise the crystal structure. The material reverts over 2–3 d to recover the original T_3R_3 crystal structure. A Rietveld refinement of this 815-atom protein by combining 3886 stereochemical restraints with a 6000-step ($d_{\min}$ = 3.06 Å) powder diffraction pattern yielded the residuals $R_{\rm wp}$ = 3.46%, R_p = 2.64%, R_F^2 = 7.10%. The demonstrated ability to solve and refine a protein crystal structure from powder diffraction data suggests that this approach can be employed, for example, to examine structural changes in a series of protein derivatives in which the structure of one member is known from a single-crystal study.

1. Introduction

The traditional uses of powder diffraction are for phase identification and quantitative phase analysis, most especially in an industrial environment (Alexander, 1976; Klug & Alexander, 1974; Jenkins & Snyder, 1996). The development of the Rietveld method, first for neutron powder diffraction data (Rietveld, 1969) and then subsequently for X-ray powder diffraction data (Young *et al.*, 1977), has lead to wide application of the technique to structure determination for complex oxides, zeolites and most recently small organic molecules (Cheetham & Taylor, 1977; Poojary & Clearfield, 1997; Harris & Tremayne, 1996). Consequently, the technique has had a significant impact on various materials sciences. Construction of high-resolution X-ray powder diffractometers (Cox *et al.*, 1986) and accurate descriptions of the diffraction line shape (Finger *et al.*, 1994) have allowed Rietveld structure refinements to rival the results commonly obtained from single-

crystal diffraction data (Dinnebier *et al.*, 1998). Recently, we have demonstrated that by combining stereochemical restraints with high-resolution X-ray powder diffraction data, a refinement of the crystal structure of a protein is feasible (Von Dreele, 1999). Here, we report the crystal structure of a new form of the T_3R_3 human insulin–zinc complex. This is the first crystal structure of a protein solved and refined from high-resolution X-ray powder diffraction data.

2. Experimental

The T_3R_3 zinc–insulin hexamer can be crystallized by the presence of 1.0 *M* NaCl in the crystallization media. The crystals are rhombohedral (space group *R*3), with unit-cell parameters a = 80.64, c = 37.78 Å, V = 213 K Å^3 and Z = 3 $Zn_2[(AB)_2]_3$. Each insulin monomer consists of an *AB* pair of polypeptide chains crosslinked by two disulfide bonds. In the T_3R_3 complex the unique crystallographic unit contains an $(AB)_2$ dimer with 810 non-H atoms (excluding solvent molecules). The first eight residues of the two *B* chains adopt different conformations, one being extended (T conformation) and the other mainly α-helical (R^f conformation; Kaarsholm *et al.*, 1989; Ciszak *et al.*, 1995; Ciszak & Smith, 1994).

In our experiments, we obtained microcrystalline powder as a slurry by grinding the T_3R_3 material with mother liquor in an agate mortar. The T_3R_3 zinc–insulin used in this work was from a ground-control sample prepared coincident with microgravity crystal-growth experiments (Smith *et al.*, 2000) aboard the US NASA Space Shuttle Discovery during its STS-95 flight mission in October 1998. The slurry was loaded

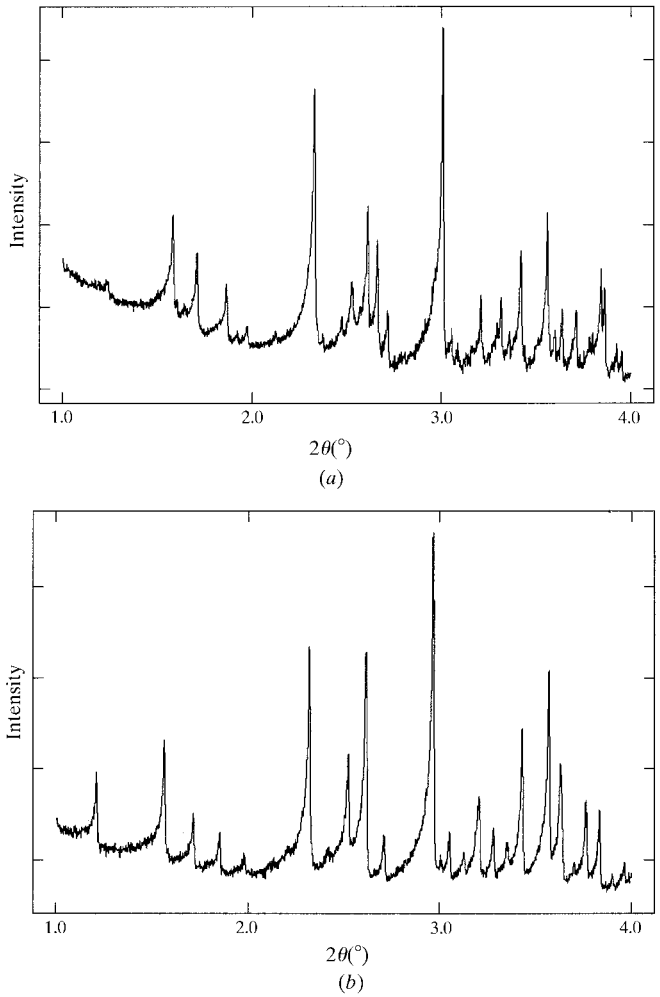

Figure 1
(*a*) High-resolution X-ray powder diffraction pattern of freshly ground Zn–human insulin complex (T_3R_3DC) taken with λ = 0.700233 Å at 2 s step^{-1} and 0.002° step^{-1}. (*b*) High-resolution X-ray powder diffraction pattern of aged Zn–human insulin complex (T_3R_3) taken with λ = 0.700233 Å; the scan shown is sum of two scans taken at 2 s step^{-1} and 0.002° step^{-1}.

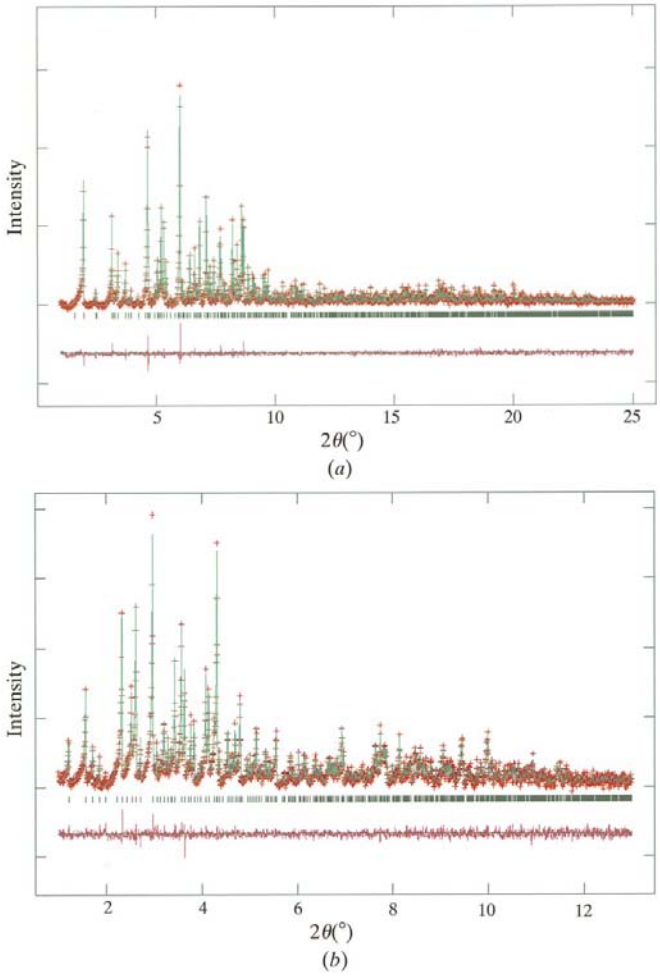

Figure 2
(*a*) High-resolution X-ray powder diffraction profile from the final Rietveld refinement of the T_3R_3DC complex. Data collected with λ = 1.401107 Å at 0.005° step^{-1}. Two scans taken at 2 s step^{-1} are summed to give this data. Observed intensities are shown in red (+), calculated and difference curves as green and magenta lines and the reflection positions are shown in black (|). The background intensity found in the refinement has been subtracted from the observed and calculated intensities for clarity. (*b*) High-resolution X-ray powder diffraction profile from the final Rietveld refinement of the T_3R_3 complex. Data collected with λ = 0.700233 Å at 0.002° step^{-1}. Two scans taken at 2 s step^{-1} are summed to give this data. Observed intensities are shown in red (+), calculated and difference curves as green and magenta lines and the reflection positions are shown in black (|). The background intensity found in the refinement has been subtracted from the observed and calculated intensities for clarity.

into a 1.5 mm diameter glass capillary and centrifuged to pack the slurry. Excess mother liquor was removed and the capillary flame-sealed to prevent subsequent solvent evaporation. Samples were ~8 mm long. X-ray powder diffraction data were then collected at room temperature on beamline X3b1 at the National Synchrotron Light Source, Brookhaven National Laboratory equipped with a double Si(111) monochromator and a Ge(111) analyser; the sample was spun during data collection to ensure good powder averaging. Details of the data collections are given in Table 1. A freshly ground sample of T_3R_3 material gave the diffraction pattern shown in Fig. 1(*a*); material which had been allowed to rest for 3 d after grinding gave a distinctly different diffraction pattern (Fig. 1*b*). A subsequent experiment in which the material was lightly crushed gave a diffraction pattern that was clearly a superposition of these two patterns; the one that matched that of the freshly ground material disappeared over the course of 2 d. The pattern from the freshly ground material was successfully indexed with program *ITO*12 (Visser, 1969) using the fitted positions of the first 25 reflections to give a rhombohedral unit cell with a = 81.275, c = 73.024 Å which is essentially a doubled c axis superlattice of the T_3R_3 structure (this phase will be denoted T_3R_3DC). The pattern from the rested material was successfully indexed using the program *DICVOL*91 (Boultif & Louër, 1991) using 24 fitted reflection positions to give a rhombohedral unit cell with a = 81.084, c = 37.537 Å, which is identical to the single-crystal unit cell for T_3R_3. The positions of the powder diffraction peaks used for indexing were obtained by fitting them to the Finger *et al.* (1994) function that describes accurately the asymmetry arising from axial divergence. Because powder pattern indexing programs are not designed to utilize the very large d spacings obtained from proteins, successful indexing was achieved by first dividing the fitted d spacings by 10; the resulting lattice parameters were multiplied by 10 to give the values shown above.

Because of the close relationship between the two phases, we attempted a structure solution of T_3R_3DC using a molecular-replacement technique adapted to powder diffraction data. A starting structural model was developed from the single-crystal coordinates for the T_3R_3 complex (Ciszak & Smith, 1994). Two T_3R_3 complexes were placed in the doubled c-axis unit cell, with one located nominally at the unit cell origin and the other at $z = \frac{1}{2}$. Initial rotations about the c axis of −15 and +15° for the two groups, respectively, were imposed for the starting position. A three-parameter (two rotation angles and one translation) rigid-body Rietveld refinement

Figure 3
The relative orientations of the human insulin peptide backbones for TR dimers in the T_3R_3 and T_3R_3DC hexamer structures. Two dimers stacked along the c axis are shown in green for T_3R_3 and in red for T_3R_3DC. The two unit-cell origins are coincident near the center of the dimers at the bottom of the figure.

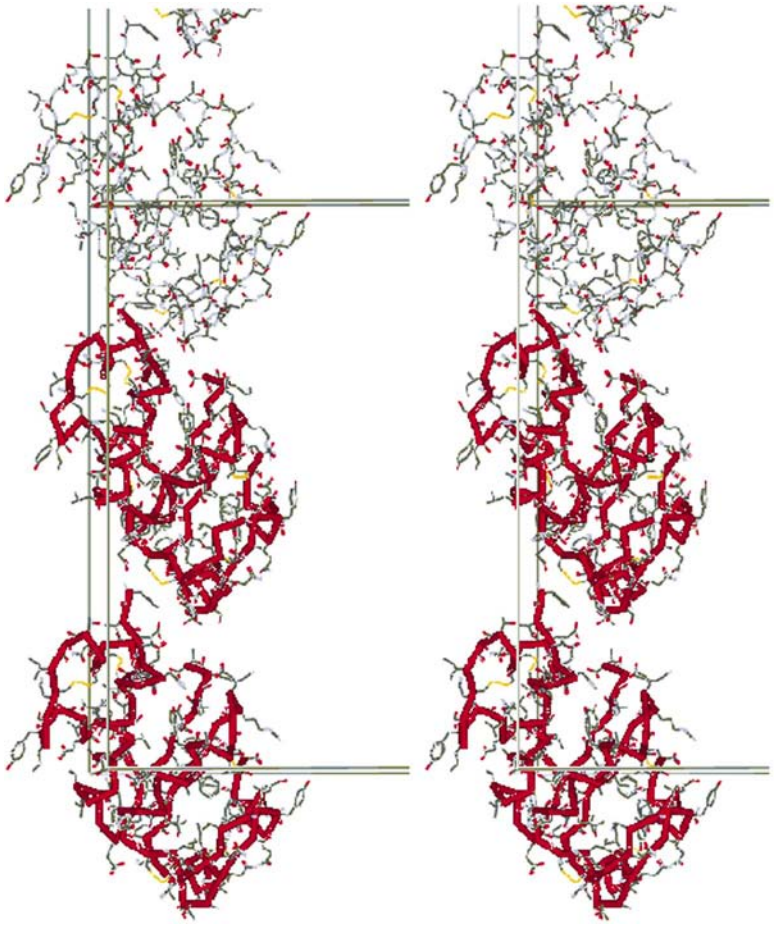

Figure 4
A stereographic packing diagram of three TR complexes stacked along the crystallographic c axis in T_3R_3DC. A Cα trace is shown in red for the two complexes that comprise the unique crystallographic unit and the unit-cell edges are also marked.

Table 1
Crystallographic and refinement data for T_3R_3 and T_3R_3DC.

Values in parentheses are estimated standard deviations in the values shown. The residuals $R_{wp} = 100\%[\sum w(I_o - I_c)^2/\sum wI_o^2]^{1/2}$, $R_p = 100\%\sum|I_o - I_c|/\sum I_o$ and $R_F^2 = 100\%\sum|F_o^2 - F_c^2|/\sum F_o^2$, where I_o and I_c are the observed and calculated powder diffraction profile intensities and w is the weight associated with I_o. F_o^2 is the value of the structure factor extracted during the Rietveld refinement and F_c^2 is the calculated structure factor. *PROCHECK* (Laskowski *et al.*, 1993) compares protein stereochemistry with expected values (Engh & Huber, 1991; Morris *et al.*, 1992).

Material	T_3R_3	T_3R_3DC
Crystal data		
Space group	*R*3	*R*3
a (Å)	80.9678 (7)	81.2780 (7)
c (Å)	37.5914 (8)	73.0389 (9)
V (Å^3)	213424 (6)	417860 (8)
PDB code	1fub	1fu2
Powder data collection		
λ (Å)	0.700233 (1)	1.401107 (1)
2θ range (°)	1.0–12.998	1.0–24.995
Δ2θ (°)	0.002	0.005
Steps	6000	4800
Combined Rietveld and stereochemical restraint refinement results		
N_{ref}	1754	2927
Resolution (Å)	33.13–3.06	50.68–3.22
$N_{restraints}$	3886	7981
N_{obs}	9886	12781
$N_{parameters}$	2459	4893
R_{wp} (%)	3.46	3.73
R_p (%)	2.64	2.84
R_F^2 (%)	7.10	8.25
Powder profile parameters		
X	0.370 (8)	0.643 (13)
X_e	0.026 (16)	−0.089 (24)
Y	2.83 (20)	5.49 (19)
Y_e	1.6 (4)	−2.60 (34)
Protein chain parameters from *PROCHECK*		
Bond error (Å)	0.006	0.006
Angle error (°)	1.39	1.37
Residues in core region (%)	91.9	87.2
ω torsion-angle error (°)	2.9	3.6
Bad contacts per 100 residues	14.0	15.9
ζ angle error (°)	2.0	1.9
Hydrogen-bond energy error (kcal mol^{-1})†	1.0	1.2
RMS deviations from planes (Å)	0.006	0.007

† 1 kcal mol^{-1} = 4.184 kJ mol^{-1}.

with a modified version of the General Structure Analysis System (*GSAS*; Larson & Von Dreele, 1986) gave smooth convergence to rotations of +9.5 and +17.2° for the two T_3R_3 complexes. The group at $z = \frac{1}{2}$ shifted in this refinement by 0.94 Å along the *c* axis. This represents a rotation of nearly 25° for one of the rigid-body groups during refinement. The final orientations of the two $(AB)_2$ complexes in the T_3R_3DC crystal structure relative to their orientations in T_3R_3 can be seen in Fig. 3. Meanwhile, the crystal structure of T_3R_3 was subjected to a combined stereochemical restraint and Rietveld refinement using techniques described previously (Von Dreele, 1999). Atom coordinates from this refinement were used to complete the rigid-body refinement of T_3R_3DC. A combined stereochemical restraint and Rietveld refinement beginning with the coordinates obtained from this final rigid-body refinement was then used to complete the structure analysis of T_3R_3DC. Protein refinement was achieved by constructing a band-diagonal approximation to the full matrix; band-matrix routines from the *SLATEC* suite (Fong *et al.*, 1993) were adapted for use in *GSAS*. A matrix bandwidth of 300 parameters was chosen for refinement of both T_3R_3 complexes. During both sets of Rietveld refinements the resulting protein stereochemistry was periodically evaluated with the *PROCHECK* (Laskowski *et al.*, 1993) suite of programs and graphically examined using the *Swiss–PdbViewer* package (Guex & Peitsch, 1999). Details of these refinements are listed in Table 1 and the resulting fitted powder diffraction profiles are shown in Figs. 2(*a*) and 2(*b*).

3. Discussion

The effect of grinding the material is to reduce its volume by 2.095% or 1490 Å^3 per T_3R_3 complex and to induce a structural change that results in a doubling of the rhombohedral unit cell along the *c* axis and is probably a consequence of simple shear. The Matthews (1976) parameter changes from 2.03 Å^3 Da^{-1} for T_3R_3 (solvent fraction 39.4%) to 1.99 Å^3 Da^{-1} for T_3R_3DC (solvent fraction 38.2%). If the phase change were simply a loss of 'liquid-like' water (29.9 Å^3 per H_2O) from the protein structure, the change would correspond to a loss of approximately 50 water molecules per T_3R_3 hexamer. A similar effect was noted previously from grinding metmyoglobin crystals (Von Dreele, 1999), although in that case no major structural change accompanied the dehydration. One of the independent dimers rotates 17.2° about the *c* axis in the conversion from T_3R_3 to T_3R_3DC; the other rotates 9.5° in the same direction. As seen in Fig. 4, this is accompanied by a collapse of the spacing between pairs of $(AB)_2$ complexes along the crystallographic *c* axis and a repositioning of one of the *B* chains that have the extended T conformation. It is likely that the water molecules expelled from the structure during grinding come from this region. A similar effect was observed in the blood-coagulation factor XIII (Weiss & Hilgenfeld, 1999), where dehydration of single crystals by exposure to PEG 6000 resulted in doubling of a monoclinic unit cell along the *c* axis accompanied by a volume reduction of 5–12%. In this structural transition one half of the factor XIII molecules rotated by 5° so that half of the original 2_1 screw axes were lost.

One of the most striking features of these powder patterns is that the diffraction lines are extremely sharp with only slight evidence of sample-dependent broadening. An analysis (Larson & Von Dreele, 1986) of the *X* and X_e profile coefficients (Table 1) gives an apparent particle size of 1.1 μm for T_3R_3 and 1.2 μm for T_3R_3DC; this corresponds to crystallites that are roughly 100 protein unit cells in extent. This is very similar to our previous result with metmyoglobin powder (Von Dreele, 1999) and sharp diffraction lines may be a typical feature of protein powder patterns. Analysis of the *Y* and Y_e profile coefficients indicate that microstrain in both T_3R_3 (0.049–0.077%) and T_3R_3DC (0.051–0.096%) is very small and slightly anisotropic. In comparison, typical microstrain broadening effects are at least an order of magnitude larger for oxides and other small structures after grinding and are caused by the introduction of point and line defects. Evidently,

annealing of protein powders occurs very rapidly at room temperature and thus point and line defects do not persist in these materials. Most impressively, there is no sign of microstrain broadening associated with the reverse conversion of T_3R_3DC to T_3R_3. It is also remarkable that simple grinding of the T_3R_3 material effected a complete conversion to the T_3R_3DC phase; there was no sign of residual T_3R_3 phase in our freshly ground samples.

The $T_3R_3 \rightarrow T_3R_3DC$ phase change and structural adjustment described above are fully consistent with results of an ongoing analysis of atomic resolution diffraction data (d_{min} = 1.2 Å) measured on cryofrozen (T = 120 K) single crystals of the T_3R_3DC form obtained from T_3R_3 single crystals grown under microgravity (Smith *et al.*, 2000). In the single-crystal case, the phase change was apparently induced by the compression arising from thermal contraction of the cryofrozen droplet of cryoprotected mother liquor surrounding the loop-mounted crystal.

In summary, we have demonstrated that it is possible to solve and refine a protein crystal structure from powder diffraction data by employing a molecular-replacement technique and a combined stereochemical restraint and Rietveld refinement. The relative ease with which this was performed here suggests that this approach can be employed, for example, to examine structural changes in a series of protein derivatives in which the structure of one member is known from a single-crystal study.

The insulin starting material for preparing the crystalline samples was biosynthetic human insulin kindly supplied by Eli Lilly Co. Crystallization and crystal-growth experiments were carried out in collaboration with Larry DeLucas and Marianna Long of the University of Alabama at Birmingham and were supported by NASA grant NCC8-12c to Larry DeLucas. RBVD acknowledges support for this work from US DOE/BES under contract W-7405-ENG-36; PWS and the SUNY X3 beamline are supported by US DOE Grant No. DE-FG02-86ER45231; GDS and RHB are grateful for support from US DHHS/PHS/NIH Grant No. GM56829.

References

Alexander, L. E. (1976). *Advances In X-ray Analysis*, edited by H. F. McMurdie, C. S. Barrett, J. B. Newkirk & C. O. Ruud, Vol. 20, pp. 1–13. New York: Plenum.
Boultif, A. & Louër, D. (1991). *J. Appl. Cryst.* **24**, 987–993.
Cheetham, A. K. & Taylor, J. C. (1977). *J. Solid State Chem.* **21**, 253–275.
Ciszak, E., Beals, J. M., Frank, B. H., Baker, J. C., Carter, N. D. & Smith, G. D. (1995). *Structure*, **6**, 615–622.
Ciszak, E. & Smith, G. D. (1994). *Biochemistry*, **33**, 1512–1517.
Cox, D. E., Hastings, J. B., Cardoso, L. P. & Finger, L. W. (1986). *Mater. Sci. Forum*, **9**, 1–20.
Dinnebier, R. E., Pink, M., Sieler, J., Norby, P. & Stephens, P. W. (1998). *Inorg. Chem.* **37**, 4996–5000.
Engh, R. A. & Huber, R. (1991). *Acta Cryst.* A**47**, 392–400.
Finger, L. W., Cox, D. E. & Jephcoat, A. P. (1994). *J. Appl. Cryst.* **27**, 892–900.
Fong, K., Jefferson, T., Suyehiro, T. & Walton L. (1993). *Guide to the SLATEC Common Mathematical Library*, http://www.netlib.org/slatec.
Guex, N. & Peitsch, M. C. (1999). *Swiss-PdbViewer*, Glaxo Wellcome Experimental Research, http://www.expasy.ch/spdbv.
Harris, K. D. M. & Tremayne, M. (1996). *Chem. Mater.* **8**, 2554–2570.
Jenkins, R. & Snyder, R. L. (1996). *Introduction to X-ray Powder Diffractometry*. New York: John Wiley.
Kaarsholm, N. C., Ko, H.-C. & Dunn, M. F. (1989). *Biochemistry*, **28**, 4427–4435.
Klug, H. P. & Alexander, L. E. (1974). *X-ray Diffraction Procedures for Polycrystalline and Amorphous Materials*. New York: John Wiley.
Larson, A. C. & Von Dreele, R. B. (1986). *General Structure Analysis System (GSAS)*, Los Alamos National Laboratory Report LAUR 86-748, ftp://ftp.lanl.gov/public/gsas.
Laskowski, R. A., MacArthur, M. W., Moss, D. S & Thornton, J. M. (1993). *J. Appl. Cryst.* **26**, 283–291.
Matthews, B. W. (1976). *J. Mol. Biol.* **33**, 491–497.
Morris, A. L., MacArthur, M. W., Hutchinson, E. G. & Thornton, J. M. (1992). *Proteins*, **12**, 345–364.
Poojary, D. M. & Clearfield, A. (1997). *Acc. Chem. Res.* **30**, 414–422.
Rietveld, H. M. (1969). *J. Appl. Cryst.* **2**, 65–71.
Smith, G. D., Blessing, R. H. & Panghorn, W. A. (2000). In preparation.
Visser, J. W. (1969). *J. Appl. Cryst.* **2**, 89–95.
Von Dreele, R. B. (1999). *J. Appl. Cryst.* **32**, 1084–1089.
Weiss, M. S. & Hilgenfeld, R. (1999). *Acta Cryst.* D**55**, 1858–1862.
Young, R. A., Mackie, P. E. & Von Dreele, R. B. (1977). *J. Appl. Cryst.* **10**, 262–269.